Optical Materials 99 (2020) 109510

Contents lists available at ScienceDirect

Optical Materials

journal homepage: http://www.elsevier.com/locate/optmat

Polarized spectral properties of Sm:$YAlO_3$ single crystal for reddish-orange laser

Bin Liu [a,b], Qingguo Wang [c], Xiaodong Xu [d,*], Jun Xu [c], Feng Zhu [b], Hang Zhou [a,**]

[a] School of Electronic and Computer Engineering, Peking University Shenzhen Graduate School, Shenzhen, 518055, China
[b] Shenzhen China Star Optoelectronics Technology Co., LTD, Shenzhen, 518107, China
[c] School of Physics Science and Engineering, Institute for Advanced Study, Tongji University, Shanghai, 200092, China
[d] Jiangsu Key Laboratory of Advanced Laser Materials and Devices, School of Physics and Electronic Engineering, Jiangsu Normal University, Xuzhou, 221116, China

ARTICLE INFO

Keywords:
Sm:$YAlO_3$
Crystal growth
Czochralski method

ABSTRACT

Sm:$YAlO_3$ (Sm:YAP) crystal with size of $\Phi 28 \times 80\ mm^3$ was grown by Czochralski (Cz) method. Polarized absorption spectra and fluorescence spectra of Sm:YAP crystal were discussed for the first time. The peak emission cross-sections were calculated to be $0.80 \times 10^{-21}\ cm^2$ (604 nm for a-polarization), $1.82 \times 10^{-21}\ cm^2$ (604 nm for b-polarization) and $1.63 \times 10^{-21}\ cm^2$ (610 nm for c-polarization), respectively. The Judd-Ofelt (JO) intensity parameters were calculated to be $\Omega_2 = 2.59 \times 10^{-20}\ cm^2$, $\Omega_4 = 1.78 \times 10^{-20}\ cm^2$ and $\Omega_6 = 2.98 \times 10^{-20}\ cm^2$, respectively. The decay lifetime of $^4G_{5/2}$ energy level was measured to be 2.51 ms. All above results indicate the Sm:YAP crystal may be a potential candidate of reddish-orange laser pumped directly by the GaN/InGaN laser diode.

1. Introduction

Visible lasers have many important applications in visible display, indoor optical communication and underwater detection [1–3]. Until a few years ago, the visible laser is generally realized through second-harmonic generation or sum frequency generation based on nonlinear crystals. The complexity and big volume of these methods restrict the applications in many areas. Fortunately, the emergence of GaN/InGaN semiconductor laser makes the direct pump of rare-earth doped crystals to be easier which significantly promotes the pumped efficiency and reduces the complexity [4].

Among rare-earth ions, trivalent praseodymium (Pr^{3+}) is the most famous one for the generation of visible lasers. But there is a minor drawback with the demand for low crystal filed strengths. Trivalent samarium (Sm^{3+}) with the corresponding emission wavelengths are close to those of Pr^{3+}-doped materials. Furthermore, the 5d-levels energetic position of Sm^{3+} is relatively higher than Pr^{3+}. Hence the excited state absorption (ESA) into 5d-levels of Sm^{3+} should be not a relatively big problem, even in a stronger crystal field material. Therefore, Sm^{3+} should be less sensitive to host materials and oxide crystals could also be considered. In addition, the upper state radiative lifetime of Sm^{3+} ($^4G_{5/2}$, in the order of a few milliseconds) is longer than that of Pr^{3+} ($^3P_0$, in the order of a few microseconds). The Sm^{3+}-doped materials are considered to be promising candidates for reddish-orange laser due to the strong emission transition of $^4G_{5/2}$-$^6H_{7/2}$ near 600 nm. So far, a lot of researches on spectroscopic characteristics of Sm^{3+}-doped crystals have been reported [5–8]. However, laser operations of Sm^{3+}-doped materials are reported rarely. In 1979, the first Sm^{3+}-based laser was realized in the Sm:TbF_3 crystal operating at 593 nm [9]. In the following, 28 mW of cw output power at 651 nm was obtained through a Sm^{3+}-doped glass fiber [2] and even 190 mW of output power corresponding to20% of slope efficiency was realized with a Sm:$LiTbF_4$ crystal emitting at 605 nm [10]. The laser operation of Sm^{3+}-doped materials were also reported in Sm:$LiLuF_4$ (Sm:LLF) and Sm:$SrAl_{12}O_{19}$ (Sm:SRA) crystals [3]. Although fluoride materials can decrease the absorption and non-radiative transitions of excited states because of the low phonon energy, the thermo-mechanical properties are poor. So it is significantly desired for new materials with both excellent thermo-mechanical properties and low phonon energy.

YAP is from the Y_2O_3–Al_2O_3 system, which owns similar physical characteristics with the famous YAG such as high mechanical hardness (Mohs hardness 8.5–9) and high thermal conductivity (~11 $W\ m^{-1}K^{-1}$ at room temperature) [11]. In addition, the phonon energy of YAP is as low as 570 cm^{-1} [11]. The excellent physical

* Corresponding author.
** Corresponding author.
E-mail addresses: xdxu79@jsnu.edu.cn (X. Xu), zhouh81@pkusz.edu.cn (H. Zhou).

https://doi.org/10.1016/j.optmat.2019.109510
Received 22 August 2019; Received in revised form 3 October 2019; Accepted 3 November 2019
Available online 8 November 2019

properties make lanthanide ions doped YAP host be widely investigated [12–18]. However, the polarized spectroscopic characteristics of Sm:YAP crystal have not been reported. In this work, XRD pattern, polarized spectral characteristics, JO theory analysis and the fluorescence lifetime of Sm:YAP crystal were discussed in detail.

2. Experiments

The Sm:YAP crystal with size of $\Phi 28 \times 80\ mm^3$ was grown by Cz method(Fig. 1). Y_2O_3, Al_2O_3 and Sm_2O_3 powders with the purity of 99.99% were used as the starting materials. They were weighed based on the formula $Sm_xY_{1-x}AlO_3$ ($x = 0.03$). After mixed completely, the powders were pressed into bulks and then sintered in air at 1300 °C for 20 h. The seed crystal was along the orientation b-axis. During the growth of Sm:YAP crystal, the pulling rate was 1 mm/h and the rotation rate was 16–20 rpm. To avoid the oxidation of Ir crucible, high-purity nitrogen gas was used as a protective atmosphere.

The structure of Sm:YAP crystal was analyzed by X-ray powder diffraction method (XRD). The XRD pattern of Sm^{3+}-doped YAP crystal is shown in Fig. 2. The diffraction peaks are in agreement with the JCPDS 11-0662. The lattice parameters of Sm:YAP crystal were calculated to be $a = 0.5228$ nm, $b = 0.7541$ nm and $c = 0.5223$ nm, similar with the pure YAP parameters of $a = 0.5330$ nm, $b = 0.7375$ nm and $c = 0.5180$ nm [19], which indicates the as-grown Sm:YAP crystal possessed the structure of orthorhombic system with the space group Pnma-D^{16}_{2h} (No.62), $Z = 4$. The sample was ground into powders and then examined on an automated Ultima IV diffractometer (Rigaku, Japan). The concentration of Sm^{3+} ions was measured by inductively coupled plasma and atomic emission spectrometry (ICPAES, Ultima2, Jobin-Yvon). The concentration of Sm^{3+} ions at the head position of Sm:$YAlO_3$ crystal was measured to be 1.9 at.% and the segregation coefficient of Sm^{3+} ions in YAP crystal was calculated to be 0.643. The concentration of Sm^{3+} ions corresponding to sample of Sm:$YAlO_3$ crystal was calculated to be 2.1 at.% (i.e. $4.2 \times 10^{20}\ cm^{-3}$). The sample with size of 7 mm × 6 mm × 5 mm, each face of which is perpendicular to one of a, b and c crystallographic direction respectively, were polished for spectroscopic experiments. The polarized absorption spectra ranged from 300 nm to 1800 nm were measured by a Spectrometer (Lambda900, PerkinElmer UV-VIS-NIR), the polarized fluorescence spectra were recorded using a Fluorescence Spectrophotometer (FSP920, Edinburgh) and the fluorescence lifetime was obtained by a spectrometer (FLS-980, Edinburgh). All the measurements of this paper were performed at room temperature.

Fig. 1. Photo of the as-grown Sm:YAP crystal.

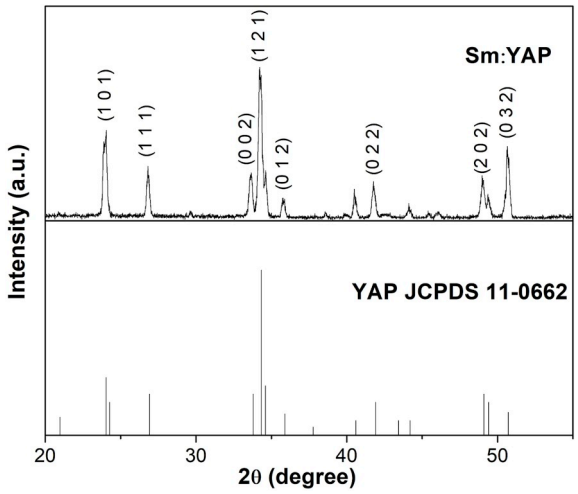

Fig. 2. XRD pattern of Sm:YAP crystal.

3. Results and discussions

3.1. Absorption spectra and JO theory analysis

The polarized absorption spectra of Sm:YAP crystal in the region of 300–1800 nm are shown in Fig. 3. It can be seen that the absorption spectra are polarization-dependent. The absorption spectra consist of eleven prominent absorption bands corresponding to the transitions from the ground state $^6H_{5/2}$ to excited states $^4K_{15/2} + {}^4H_{11/2,9/2,7/2} + {}^4D_{7/2}$, $^4F_{9/2} + ({}^4D, {}^6P)_{5/2} + {}^4D_{3/2}$, $^4K_{13/2} + {}^4L_{17/2} + {}^6P_{7/2} + {}^4D_{1/2}$, $^4G_{11/2} + {}^4L_{15/2} + {}^4K_{11/2} + {}^6P_{3/2} + {}^4F_{7/2} + {}^4L_{13/2} + ({}^6P, {}^4P)_{5/2}$, $^4F_{5/2} + {}^4I_{15/2} + {}^4G_{9/2} + {}^4M_{17/2}$, $^4G_{7/2} + {}^4I_{9/2} + {}^4M_{15/2} + {}^4I_{11/2} + {}^4I_{13/2}$, $^6F_{11/2}$, $^6F_{9/2}$, $^6F_{7/2}$, $^6F_{5/2}$, and $^6F_{3/2} + {}^6H_{15/2} + {}^6F_{1/2}$, respectively. The polarized absorption spectra between 520 nm and 880 nm is omitted because the absorption band around 565 nm is too weak to be observed. Some absorption bands are difficult to be resolved fully due to the interaction with each other, in other words the crystal-field splitting of neighboring transitions is relatively larger than that of their energy levels [20]. In the visible region, the most intense absorption peaks of Sm^{3+} ions for three polarizations are all located at 409 nm which is suitable for pumping by GaN/InGaN laser diode. The corresponding absorption cross sections for a, b and c polarization are $0.50 \times 10^{-20}\ cm^2$, $1.34 \times 10^{-20}\ cm^2$ and $1.72 \times 10^{-20}\ cm^2$ with the full width at half maxim (FWHM) of 8.4 nm,

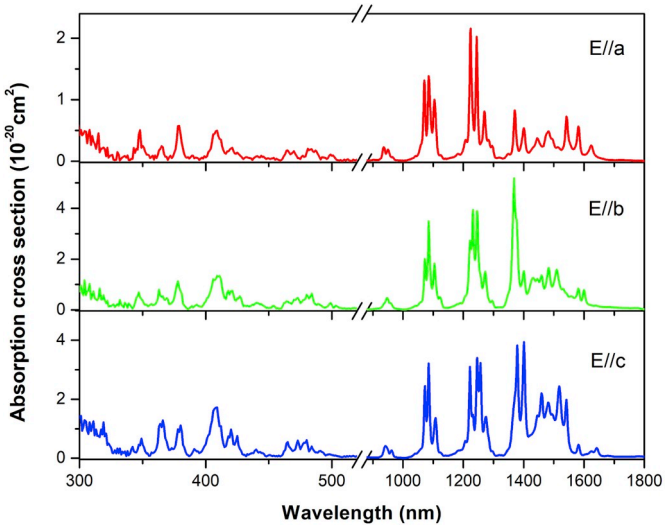

Fig. 3. Polarized absorption spectra of Sm:YAP crystal.

10.2 nm and 9.4 nm, respectively. The absorption cross sections of Sm:YAP crystal are comparable with that of Sm:$LiYF_4$ (0.72×10^{-20} cm^2 for σ-polarization, 1.37×10^{-20} cm^2 for π-polarization) [8].

The radiative transition of a lanthanide ion corresponding to the $4f^N$ configuration could be analyzed using the JO theory [21,22]. In this work, nine absorption bands were used to calculate the JO intensity parameters and the detailed procedures were same with other literatures [23]. The parameters such as the refractive index n of Sm:YAP crystal was estimated from Ref. [24] and the reduced matrix elements $\langle||U^{(t)}||\rangle$ between ground and excited states were adopted from Ref. [25]. The refractive index n, the calculated line strength S_{cal}, the experimental line strength S_{exp} together with mean wavelength $\bar{\lambda}$ are listed in Table 1. The RMS deviations corresponding to a, b and c polarization were calculated to be 2.08×10^{-22} cm^2, 3.88×10^{-22} cm^2 and 1.96×10^{-22} cm^2, respectively. The relatively low values of rmsΔS indicate that the fitting JO parameters could be considered reasonable.

Three JO intensity parameters corresponding to a, b and c polarization were obtained by the least-square fitting between experimental line strength S_{exp} and calculated line strength S_{cal}. For the biaxial Sm:YAP crystal, the effective J-O intensity parameters can be calculated by $\Omega_{t,eff} = (\Omega_{t,a} + \Omega_{t,b} + \Omega_{t,c})/3$ [26]. The effective J-O parameters of Sm:YAP crystal were obtained to be $\Omega_{2,eff} = 2.59 \times 10^{-20}$ cm^2, $\Omega_{4,eff} = 1.78 \times 10^{-20}$ cm^2 and $\Omega_{6,eff} = 2.98 \times 10^{-20}$ cm^2, respectively. The J-O intensity parameters of Sm^{3+}-doped different crystals are listed in Table 2. The parameter Ω_2 is closely related to the asymmetry and contravalency of the rare-earth element sites. In this work, the value 2.59×10^{-20} cm^2, which is lower than that of $CaGdAlO_4$ and $CaNb_2O_6$ but higher than that of $LiLuF_4$ and $LiYF_4$, indicates that grade of contravalency between the Sm^{3+} ions and the neighboring O^{2-} ions of YAP is lower than that of $CaGdAlO_4$ and $CaNb_2O_6$ but higher than $LiLuF_4$ and $LiYF_4$ [27].

The calculated radiative probability $A(J, J')$, fluorescent branching ratio $\beta_{JJ'}$ and the radiative lifetime τ_{rad} are summarized in Table 3. The parameters of fluorescence branching ratio $\beta_{JJ'}$ and radiative lifetime τ_{rad} are related to the laser power of potential emission transition. The high value of $\beta_{JJ'}$ generally indicates the high possibility of laser operation. The $^4G_{5/2} \rightarrow {}^6H_{7/2}$ transition owns the highest fluorescence branching ratio of 36.08%, 51.35% and 38.13% for a, b and c polarization, respectively. The branching radio of $^4G_{5/2} \rightarrow {}^6H_{7/2}$ transition in Sm:$LiLuF_4$ was 44.57% and efficient laser operation of $^4G_{5/2} \rightarrow {}^6H_{7/2}$ transition was obtained [3,7], which indicated that $^4G_{5/2} \rightarrow {}^6H_{7/2}$ transition of Sm:YAP crystal may be a promising channel for the generation of reddish-orange laser. The corresponding radiative lifetime τ_{rad} is 3.31 ms which is obviously longer than that of Sm:CGA (1.22 ms) [5] and Sm:$LiNbO_3$ (1.12 ms) [20].

Table 2
The JO intensity parameters of Sm:YAP crystals.

Crystals		$\Omega_2(10^{-20}\,cm^2)$	$\Omega_4(10^{-20}\,cm^2)$	$\Omega_6(10^{-20}cm^2)$	Ref.
$CaNb_2O_6$		6.33	6.49	3.72	[23]
$LiLuF_4$		1.39	3.45	2.66	[7]
$CaGdAlO_4$		3.00	6.10	6.50	[5]
$LiYF_4$		0.55	2.44	1.72	[8]
YAP	$\Omega_{t,a}$	2.04	0.45	1.87	This work
	$\Omega_{t,b}$	2.23	2.68	3.57	
	$\Omega_{t,c}$	3.50	2.20	3.50	
	$\Omega_{t,eff}$	2.59	1.78	2.98	

3.2. Fluorescence spectra

The polarized fluorescence spectra of Sm:YAP crystal are shown in Fig. 4. In the visible region, the transitions of Sm^{3+} ions are from the $^4G_{5/2}$ multiplet and four principle emission bands of $^4G_{5/2} \rightarrow {}^6H_{5/2}$, $^4G_{5/2} \rightarrow {}^6H_{7/2}$, $^4G_{5/2} \rightarrow {}^6H_{9/2}$ and $^4G_{5/2} \rightarrow {}^6H_{11/2}$ are marked. As we can see that emission spectra are polarization dependent, which the peak locations and intensities are different with each other for a, b and c polarization, due to the anisotropy of YAP crystal [16]. The peak wavelength, FWHM and stimulated emission cross-section for three polarizations are listed in Table 4. The maximum emission cross-sections corresponding to the transition $^4G_{5/2} \rightarrow {}^6H_{7/2}$ are 0.80×10^{-21} cm^2 at 604 nm for a-polarization, 1.82×10^{-21} cm^2 at 604 nm for b-polarization and 1.63×10^{-21} cm^2 at 610 nm for c-polarization. The product of the radiative lifetime of $^4G_{5/2}$ multiplet and emission cross-section corresponding to $^4G_{5/2} \rightarrow {}^6H_{7/2}$ transition for b-polarization is 6.02×10^{-21} cm^2 ms (2.65×10^{-21} cm^2 ms for a-polarization and 5.40×10^{-21} cm^2 ms for c-polarization), inversely proportional to the threshold of laser operation, comparable with that of Sm:$LiYF_4$ (4.69×10^{-21} cm^2 ms for σ-polarization and 7.17×10^{-21} cm^2 ms for π-polarization) [8] and Sm:$LiLuF_4$ (3.03×10^{-21} cm^2 ms for σ-polarization and 6.54×10^{-21} cm^2 ms for π-polarization) [7]. The results show that laser threshold corresponding to $^4G_{5/2} \rightarrow {}^6H_{7/2}$ transition of Sm:YAP crystal is almost the same with Sm:$LiYF_4$ and Sm:$LiLuF_4$. As we all know, physical characteristics of fluoride materials such as mechanical hardness and thermal conductivity are relatively low. However, the excellent thermo-mechanical characteristics are essential for the stability of laser output. The Sm:YAP crystal, owning similar physical characteristics with the famous YAG and similar phonon energy with the fluoride materials, is favorable for the stable laser operation. The above results make Sm:YAP crystal to be a promising candidate for reddish-orange laser operation.

The fluorescence decay curve corresponding to $^4G_{5/2} \rightarrow {}^6H_{7/2}$

Table 1
The calculated average wavelength $\bar{\lambda}$, refractive index n, experimental line strength $S_{exp}(J, J')$ and calculated line strength $S_{cal}(J, J')$ of Sm^{3+} ions in YAP crystal.

Excited state $^6H_{5/2}$	E//a				E//b				E//c			
	$\bar{\lambda}$ (nm)	n	S_{exp} (10^{-20} cm^2)	S_{cal} (10^{-20} cm^2)	$\bar{\lambda}$ (nm)	n	S_{exp} (10^{-20} cm^2)	S_{cal} (10^{-20} cm^2)	$\bar{\lambda}$ (nm)	n	S_{exp} (10^{-20} cm^2)	S_{cal} (10^{-20} cm^2)
$^4K_{13/2}+{}^4L_{17/2}+{}^6P_{7/2}+{}^4D_{1/2}$	379	1.992	0.129	0.144	378	1.983	0.273	0.279	379	1.966	0.281	0.273
$^4G_{11/2}+{}^4L_{15/2}+{}^4K_{11/2}+{}^6P_{3/2}+{}^4F_{7/2}+{}^4L_{13/2}+{}^6P_{5/2}+{}^4P_{5/2}$	407	1.983	0.167	0.128	407	1.973	0.557	0.619	407	1.958	0.508	0.520
$^4F_{5/2}+{}^4I_{15/2}+{}^4G_{9/2}+{}^4M_{17/2}$	420	1.979	0.014	0.017	419	1.970	0.064	0.034	419	1.955	0.062	0.033
$^4G_{7/2}+{}^4I_{9/2}+{}^4M_{15/2}+{}^4I_{11/2}+{}^4I_{13/2}$	481	1.966	0.142	0.135	476	1.957	0.299	0.264	476	1.943	0.278	0.260
$^6F_{11/2}$	948	1.936	0.097	0.096	948	1.927	0.159	0.186	948	1.916	0.161	0.182
$^6F_{9/2}$	1085	1.933	0.662	0.646	1088	1.925	1.268	1.274	1081	1.913	1.241	1.241
$^6F_{7/2}$	1239	1.932	0.863	0.871	1240	1.923	1.935	1.924	1244	1.912	1.842	1.829
$^6F_{5/2}$	1381	1.931	0.173	0.194	1373	1.922	0.881	0.835	1386	1.911	0.759	0.742
$^6F_{3/2}+{}^6H_{15/2}+{}^6F_{1/2}$	1519	1.930	0.762	0.758	1501	1.922	1.132	1.134	1495	1.910	1.506	1.501

Table 3
The radiative transition rates $A(J,J')$, branching ratios $\beta_{JJ'}$ and radiative lifetime τ_{rad} of Sm:YAP crystal.

Transitions from $^4G_{5/2}$	$A_{ed}(s^{-1})$	E//a $A_{md}(s^{-1})$	β(%)	$A_{ed}(s^{-1})$	E//b $A_{md}(s^{-1})$	β(%)	$A_{ed}(s^{-1})$	E//c $A_{md}(s^{-1})$	β(%)
$^6F_{11/2}$	0.270	0	0.09	0.521	0	0.16	0.241	0	0.08
$^6F_{9/2}$	1.959	0	0.67	1.147	0	0.35	1.589	0	0.55
$^6F_{7/2}$	0.790	1.906	0.93	1.207	1.941	0.97	1.629	1.906	1.21
$^6F_{5/2}$	13.931	6.109	6.88	6.270	6.124	3.80	11.369	6.012	5.97
$^6F_{3/2}$	2.388	9.029	3.92	0.989	8.855	3.02	1.773	8.692	3.59
$^6H_{15/2}$	0.425	0	0.15	0.762	0	0.23	0.314	0	0.11
$^6F_{1/2}$	2.498	0	0.86	0.995	0	0.31	1.768	0	0.61
$^6H_{13/2}$	5.708	0	1.96	10.906	0	3.34	4.799	0	1.65
$^6H_{11/2}$	15.197	0	5.22	25.178	0	7.72	22.089	0	7.58
$^6H_{9/2}$	94.103	0	32.31	63.639	0	19.52	85.055	0	29.19
$^6H_{7/2}$	81.736	23.369	36.08	144.258	23.170	51.35	88.953	22.145	38.13
$^6H_{5/2}$	4.179	27.688	10.94	2.791	27.309	9.23	5.507	27.497	11.33
Radiative lifetime (ms)	τ_{rad} = 3.31								

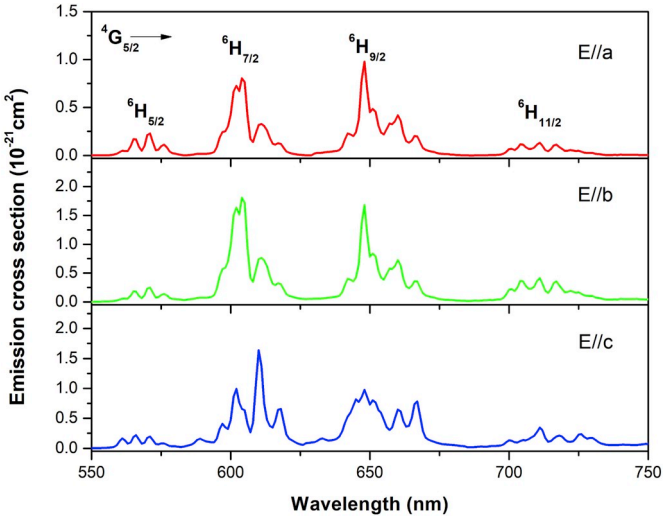

Fig. 4. Polarized fluorescence spectra of Sm:YAP crystal.

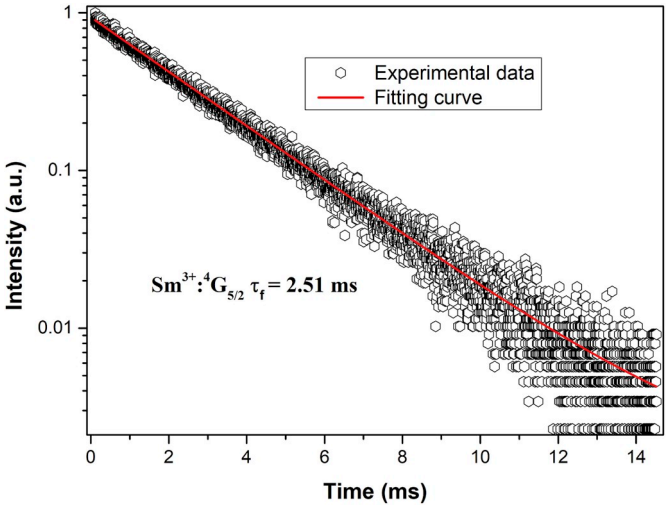

Fig. 5. Decay curve of the $^4G_{5/2}$ level of Sm:YAP crystal.

Table 4
The emission peak wavelength λ, FWHM and emission cross section σ_{em} corresponding to each polarization of Sm:YAP crystal.

Transition $^4G_{5/2}$ →	Polarization	Peak wavelength (nm)	FWHM (nm)	σ_{em} (10^{-21}cm^2)
$^6H_{5/2}$	a	571	3.01	0.24
	b	571	3.16	0.25
	c	566	3.28	0.22
$^6H_{7/2}$	a	604	6.29	0.80
	b	604	6.32	1.82
	c	610	3.26	1.63
$^6H_{9/2}$	a	648	3.50	0.99
	b	648	2.55	1.69
	c	648	4.21	0.99
$^6H_{11/2}$	a	711	3.84	0.14
	b	711	4.15	0.43
	c	711	4.17	0.36

transition under excitation at 409 nm, analyzed by a single exponential model, is shown in Fig. 5. The fluorescence lifetime τ_f was obtained to be 2.51 ms. The value of τ_f is lower than the calculated radiative lifetime τ_{rad} (3.31 ms) because of the high Sm^{3+} ions concentration. The Sm^{3+} ions concentration (4.2×10^{20} cm^{-3}) in Sm:YAP is larger than 4×10^{20} cm^{-3} in which energy transfer via cross-relaxation will decrease the decay lifetime of $^4G_{5/2}$ multiplet significantly [4]. The similar phenomenon was also reported in the Sm:BOTS glass [28] and Sm:LGT glass [29]. In other words, low fluorescence quantum efficiency doesn't mean the laser oscillation is impossible. For example, although the concentration quenching effect of Nd^{3+} ions was reported for highly concentration doping, the Nd:YAG ceramics [30] has still been testified to be a high-efficiency laser material. The above results indicate Sm:YAP crystal is a potential candidate of reddish-orange laser pumped by InGaN laser diode.

3.3. Comparison with other crystal

A comparison of spectroscopic parameters for Sm^{3+}-doped YAP and other common host materials for visible laser is presented in Table 5. Sm:YAP crystal possesses higher emission cross-section than that of Sm:$SrAl_{12}O_{19}$, Sm:$LiLuF_4$ and Sm:$LiYF_4$ which have been consider to be remarkable laser materials. The absorption cross-sections of Sm:YAP are comparable with Sm:$LiLuF_4$ and Sm:$LiYF_4$, while the corresponding absorption band widths of Sm^{3+}-doped YAP are bigger than that of $LiLuF_4$ and $LiYF_4$ which is more favorable for the pump of InGaN laser diode. The fluorescence lifetime of Sm:YAP is in the same order with Sm^{3+}-doped other materials. As depicted in part 3.2, the lifetime is relevant to the concentration of Sm^{3+} ions and it would be improved by decreasing the doped concentration. All the results demonstrate that Sm:YAP is a potential candidate for reddish-orange laser operation.

4. Conclusions

Sm:YAP single crystal with size of $\Phi 28 \times 80$ mm^3 was grown using

Table 5
Comparison between Sm:YAP crystal and other crystal doped with Sm^{3+}.

Properties	$LiYF_4$	$LiLuF_4$	$SrAl_{12}O_{19}$	YAP
Absorption peak wavelength (nm) ($^6H_{5/2} \rightarrow {}^4F_{7/2}$)	401(σ) 401(π)	401(σ) 401(π)	400(σ)	409(E//a) 409(E//b) 409(E//c)
Absorption cross-section ($10^{-20}cm^2$)	0.72(σ) 1.37(π)	1.04(σ) 1.51(π)	8.5(σ)	0.50 (E//a) 1.34 (E//b) 1.72 (E//c)
Absorption bandwidth (FWHM) (nm)	3(σ) 2(π)	2.3(σ) 3.1(π)	–	8.4(E//a) 10.2 (E//b) 9.4(E//c)
Emission peak wavelength (nm) ($^4G_{5/2} \rightarrow {}^6H_{7/2}$)	598(σ) 605(π)	598(σ) 605(π)	593(σ)	604(E//a) 604(E//b) 610(E//c)
Emission cross-section ($10^{-21}cm^2$)	0.679 (σ) 1.039 (π)	0.659 (σ) 1.421 (π)	1.2(σ)	0.80 (E//a) 1.82 (E//b) 1.63 (E//c)
Fluorescence bandwidth (FWHM) (nm)	7.5(σ) 9.5(π)	7.5(σ) 9.5(π)	–	6.29 (E//a) 6.32 (E//b) 3.26 (E//c)
Fluorescence lifetime (ms)	4.80	2.65	3.40	2.51
References	[8]	[7]	[3]	This work

the Cz method. The polarized spectra properties of Sm:YAP crystal were reported for the first time. The peak absorption cross-sections corresponding to a, b and c polarization were obtained to be $0.50 \times 10^{-20}\ cm^2$, $1.34 \times 10^{-20}\ cm^2$ and $1.72 \times 10^{-20}\ cm^2$, respectively. Based on JO theory, intensity parameters were fitted to be $\Omega_2 = 2.59 \times 10^{-20}\ cm^2$, $\Omega_4 = 1.78 \times 10^{-20}\ cm^2$ and $\Omega_6 = 2.98 \times 10^{-20}\ cm^2$, respectively. In addition, the emission cross-sections were calculated to be $0.80 \times 10^{-21}\ cm^2$ at 604 nm for a-polarization, $1.82 \times 10^{-21}\ cm^2$ at 604 nm for b-polarization and $1.63 \times 10^{-21}\ cm^2$ at 610 nm for c-polarization, respectively. The decay lifetime of $^4G_{5/2}$ multiplet was measured to be 2.51 ms. All the above results illustrate that Sm:YAP is a potential candidate for reddish-orange laser pumped directly by InGaN LD.

Declaration of competing interest

The authors declare that they have no known competing financial interests or personal relationships that could have appeared to influence the work reported in this paper.

Acknowledgments

This research is partially supported by the National Key Research and Development Program of China (No. 2016YFB0701002), National Natural Science Foundation of China (No. 61621001, 51672190, 61605069), Postdoctoral Science Foundation of China (No. 2019M650332), State Key Laboratory of Crystal Materials of Shandong University, Shanghai Engineering Research Center for Sapphire Crystals (No.14DZ2252500), and Shenzhen China Star Optoelectronics Technology Co., LTD.

References

[1] Q.N. Fang, D.Z. Lu, H.H. Yu, H.J. Zhang, J.Y. Wang, Self-frequency-doubled vibronic yellow Yb: YCOB laser at the wavelength of 570 nm, Opt. Lett. 41 (2016) 1002–1005.
[2] X.D. Xu, Z.W. Hu, R.J. Li, D.Z. Li, J.Q. Di, L.B. Su, Q.H. Yang, Q.L. Sai, H.L. Tang, Q. G. Wang, A. Strzep, J. Xu, Optical spectroscopy of Dy^{3+}-doped $CaGdAlO_4$ single crystal for potential use in solid-state yellow lasers, Opt. Mater. 66 (2017) 469–473.
[3] D.T. Marzahl, P.W. Metz, C. Kränkel, G. Huber, Spectroscopy and laser operation of Sm^{3+}-doped lithium lutetium tetrafluoride ($LiLuF_4$) and strontium hexaaluminate ($SrAl_{12}O_{19}$), Opt. Express 23 (2015) 21118–21127.
[4] C. Kränkel, D.T. Marzahl, F. Moglia, G. Huber, P.W. Metz, Out of the blue: semiconductor laser pumped visible rare-earth doped lasers, Laser Photonics Rev. 10 (2016) 548–568.
[5] X.D. Xu, Z.W. Hu, R.J. Li, D.Z. Li, J.Q. Di, L.B. Su, Q.H. Yang, Q.L. Sai, H.L. Tang, Q. G. Wang, A. Strzep, J. Xu, Polarized spectral properties of Sm: $CaGdAlO_4$ crystal for reddish-orange laser, Opt. Mater. 69 (2017) 333–338.
[6] D. Pugh-Thomas, Spectroscopic properties and Judd–Ofelt analysis of BaY_2F_8:Sm^{3+}, J. Opt. Soc. Am. B 31 (2014) 1777–1785.
[7] G.Q. Wang, X.H. Gong, Y.F. Lin, Y.J. Chen, J.H. Huang, Z.D. Luo, Y.D. Huang, Polarized spectral properties of Sm^{3+}:$LiLuF_4$ crystal for visible laser application, Opt. Mater. 37 (2014) 229–234.
[8] G.Q. Wang, Y.F. Lin, X.H. Gong, Y.J. Chen, J.H. Huang, Z.D. Luo, Y.D. Huang, Polarized spectral properties of Sm^{3+}:$LiYF_4$ crystal, J. Lumin. 147 (2014) 23–26.
[9] B.N. Kazakov, M.S. Orlov, M.V. Petrov, A.L. Stolov, A.M. Tkachuk, Induced emission of Sm^{3+} ions in the visible region of the spectrum, Opt Spectrosc. 47 (1979) 676–677.
[10] H.P. Jenssen, J. Eichenholz, M. Richardson, Visible (orange) laser emission from Sm doped $LiTbF_4$, Adv. Solid State Lasers Tech. Dig. (1995). ME2-1/73–75.
[11] A.A. Kaminskii, Crystalline Lasers: Physical Processes and Operating Schemes, CRC Press, United States, 1996.
[12] V.E. Kisel, S.V. Kurilchik, A.S. Yasukevich, S.V. Grigoriev, S.A. Smirnova, N. V. Kuleshov, Spectroscopy and femtosecond laser performance of Yb^{3+}:$YAlO_3$ crystal, Opt. Lett. 33 (2008) 2194–2196.
[13] Y.H. Zong, G.J. Zhao, J. Zhu, J. Xu, Growth and its spectroscopic properties of Sm: YAP crystal, J. Cryst. Growth 291 (2006) 468–471.
[14] Y.L. Lu, Y.B. Dai, Y. Yang, J. Wang, A.P. Dong, B.D. Sun, Anisotropy of thermal and spectral characteristics in Tm:YAP laser crystals, J. Alloy. Comp. 453 (2008) 482–486.
[15] Y. Wang, J.F. Li, Z.J. Zhu, Z.Y. You, J.L. Xu, C.Y. Tu, Mid-infrared emission in Dy: $YAlO_3$ crystal, Opt. Mater. Express 4 (2014) 1104–1111.
[16] T. Danger, A. Bleckmann, G. Huber, Stimulated emission and laser action of Pr^{3+}-doped $YA1O_3$, Appl. Phys. B Laser Opt. 58 (1994) 413–420.
[17] G.C. Kim, H.L. Park, T.W. Kim, Emission color tuning from blue to green through cross-relaxation in heavily Tb^{3+}-doped $YAlO_3$, Mater. Res. Bull. 36 (2001) 1603–1608.
[18] H. Gao, Y. Wang, Photoluminescence of Eu^{3+} activated $YAlO_3$ under UV–VUV excitation, Mater. Res. Bull. 42 (2007) 921–927.
[19] R. Diehl, G. Brandt, Crystal structure refinement of $YAlO_3$, a promising laser material, Mater. Res. Bull. 10 (1975) 85–90.
[20] G. Dominiak-Dzik, Sm^{3+}-doped $LiNbO_3$ crystal, optical properties and emission cross-sections, J. Alloy. Comp. 391 (2005) 26–32.
[21] B.R. Judd, Optical absorption intensities of rare-earth ions, Phys. Rev. 127 (1962) 750–761.
[22] G.S. Ofelt, Intensities of crystal spectra of rare-earth ions, J. Chem. Phys. 37 (1962) 511–520.
[23] J.Q. Di, X.D. Xu, C.T. Xia, H.D. Zeng, Y. Cheng, D.Z. Li, D.H. Zhou, F. Wu, J. M. Cheng, J. Xu, Crystal growth and optical properties of Sm:$CaNb_2O_6$ single crystal, J. Alloy. Comp. 536 (2012) 20–25.
[24] M.J. Weber, B.H. Matsinger, V.L. Donlan, G.T. Surratt, Optical transition probabilities for trivalent holmium in LaF_3 and $YAlO_3$, J. Chem. Phys. 57 (1972) 562–567.
[25] W.T. Carnall, P.R. Fields, K. Rajnak, Electronic energy levels in the trivalent lanthanide aquo ions. I. Pr^{3+}, Nd^{3+}, Pm^{3+}, Sm^{3+}, Dy^{3+}, Ho^{3+}, Er^{3+}, and Tm^{3+}, J. Chem. Phys. 49 (1968) 4424–4442.
[26] Z.D. Luo, X.Y. Chen, T.J. Zhao, Judd-Ofelt parameter analysis of rare earth anisotropic crystals by three perpendicular unpolarized absorption measurements, Opt. Commun. 134 (1997) 415–422.
[27] C.K. Jørgensen, R. Reisfeld, Judd-Ofelt parameters and chemical bonding, J. Less Common Met. 93 (1983) 107–112.
[28] K. Maheshvaran, K. Linganna, K. Marimuthu, Composition dependent structural and optical properties of Sm^{3+} doped boro-tellurite glasses, J. Lumin. 131 (2011) 2746–2753.
[29] M. Jayasimhadri, E.J. Cho, K.W. Jang, H.S. Lee, S.I. Kim, Spectroscopic properties and Judd–Ofelt analysis of Sm^{3+} doped lead–germanate–tellurite glasses, J. Phys. D Appl. Phys. 41 (2008) 175101–175107.
[30] J. Lu, M. Prabhu, J. Xu, K.I. Ueda, H. Yagi, T. Yanagitani, A.A. Kaminskii, Highly efficient 2% Nd:yttrium aluminum garnet ceramic laser, Appl. Phys. Lett. 77 (2000) 3707–3709.